

University of Groningen

## Covalent bond force profile and cleavage in a single polymer chain

Garnier, L.; Gauthier-Manuel, B.; van der Vegte, E. W.; Snijders, J. G.; Hadziioannou, G.

*Published in:*  
Journal of Chemical Physics

*DOI:*  
[10.1063/1.482068](https://doi.org/10.1063/1.482068)

**IMPORTANT NOTE: You are advised to consult the publisher's version (publisher's PDF) if you wish to cite from it. Please check the document version below.**

*Document Version*  
Publisher's PDF, also known as Version of record

*Publication date:*  
2000

[Link to publication in University of Groningen/UMCG research database](#)

*Citation for published version (APA):*

Garnier, L., Gauthier-Manuel, B., van der Vegte, E. W., Snijders, J. G., & Hadziioannou, G. (2000). Covalent bond force profile and cleavage in a single polymer chain. *Journal of Chemical Physics*, 113(6), 2497 - 2503. [PII [S0021-9606(00)50530-3]]. <https://doi.org/10.1063/1.482068>

### Copyright

Other than for strictly personal use, it is not permitted to download or to forward/distribute the text or part of it without the consent of the author(s) and/or copyright holder(s), unless the work is under an open content license (like Creative Commons).

The publication may also be distributed here under the terms of Article 25fa of the Dutch Copyright Act, indicated by the "Taverne" license. More information can be found on the University of Groningen website: <https://www.rug.nl/library/open-access/self-archiving-pure/taverne-amendment>.

### Take-down policy

If you believe that this document breaches copyright please contact us providing details, and we will remove access to the work immediately and investigate your claim.

*Downloaded from the University of Groningen/UMCG research database (Pure): <http://www.rug.nl/research/portal>. For technical reasons the number of authors shown on this cover page is limited to 10 maximum.*

## Covalent bond force profile and cleavage in a single polymer chain

Lionel Garnier, Bernard Gauthier-Manuel, Eric W. van der Vegte, Jaap Snijders, and Georges Hadziioannou

Citation: *J. Chem. Phys.* **113**, 2497 (2000); doi: 10.1063/1.482068

View online: <https://doi.org/10.1063/1.482068>

View Table of Contents: <http://aip.scitation.org/toc/jcp/113/6>

Published by the [American Institute of Physics](#)

---

### Articles you may be interested in

[The mechanical strength of a covalent bond calculated by density functional theory](#)

*The Journal of Chemical Physics* **112**, 7307 (2000); 10.1063/1.481330

[Calibration of atomic-force microscope tips](#)

*Review of Scientific Instruments* **64**, 1868 (1993); 10.1063/1.1143970

[A density functional theory model of mechanically activated silyl ester hydrolysis](#)

*The Journal of Chemical Physics* **140**, 044321 (2014); 10.1063/1.4862827

[Dielectric elastomers of interpenetrating networks](#)

*Applied Physics Letters* **95**, 232909 (2009); 10.1063/1.3272685

---

PHYSICS TODAY

WHITEPAPERS

#### ADVANCED LIGHT CURE ADHESIVES

Take a closer look at what these environmentally friendly adhesive systems can do

READ NOW

PRESENTED BY  
 **MASTERBOND**  
ADHESIVES | SEALANTS | COATINGS

# Covalent bond force profile and cleavage in a single polymer chain

Lionel Garnier

*Department of Polymer Chemistry and Materials Science Centre, Rijksuniversiteit Groningen, Nijenborgh 4, 9747 AG Groningen, The Netherlands and Laboratoire de Physique et Métrologie des Oscillateurs du CNRS associé à l'Université de Franche-Comté, JMFC FRW 0067, 25030 Besancon Cedex, France*

Bernard Gauthier-Manuel<sup>a)</sup>

*Laboratoire de Physique et Métrologie des Oscillateurs du CNRS associé à l'Université de Franche-Comté, JMFC FRW 0067, 25030 Besancon Cedex, France*

Eric W. van der Vegte

*Department of Polymer Chemistry and Materials Science Centre, Rijksuniversiteit Groningen, Nijenborgh 4, 9747 AG Groningen, The Netherlands*

Jaap Snijders

*Theoretical Chemistry, Materials Science Centre, Rijksuniversiteit Groningen, Nijenborgh 4, 9747 AG Groningen, The Netherlands*

Georges Hadziioannou<sup>a)</sup>

*Department of Polymer Chemistry and Materials Science Centre, Rijksuniversiteit Groningen, Nijenborgh 4, 9747 AG Groningen, The Netherlands*

(Received 17 March 2000; accepted 9 May 2000)

We present here the measurement of the single-polymer entropic elasticity and the single covalent bond force profile, probed with two types of atomic force microscopes (AFM) on a synthetic polymer molecule: polymethacrylic acid in water. The conventional AFM allowed us to distinguish two types of interactions present in this system when doing force spectroscopic measurements: the first interaction is associated with adsorption sites of the polymer chains onto a bare gold surface, the second interaction is directly correlated to the rupture process of a single covalent bond. All these bridging interactions allowed us to stretch the single polymer chain and to determine the various factors playing a role in the elasticity of these molecules. To obtain a closer insight into the bond rupture process, we moved to a force sensor stable in position when measuring attractive forces. By optimizing the polymer length so as to fulfill the elastic stability conditions, we were able for the first time to map out the entire force profile associated with the cleavage of a single covalent bond. Experimental data coupled with molecular quantum mechanical calculations strongly suggest that the breaking bond is located at one end of the polymer chain. © 2000 American Institute of Physics. [S0021-9606(00)50530-3]

## I. INTRODUCTION

In complex systems such as synthetic and natural polymers, the challenge is to measure and evaluate their properties at the molecular scale and to relate these to the structures at various length scales and to macroscopic properties. Polymer materials are known for their rich structural and mechanical behavior originating from their macromolecular nature. The system we used in this study consists of a self-assembling mixed monolayer of 12-mercapto-1-dodecanol and polymethacrylic acid ( $\bar{N}_w/\bar{N}_n \approx 2$ ) substituted at both ends with a thiol group (HS-PMAA-SH). This system was probed with two types of atomic force microscope (AFM). The conventional AFM, with a soft cantilever (0.07 N/m), is well known for its good force resolution ( $<100$  pN), allowing the investigation of an individual molecule's properties, such as entropic elasticity,<sup>1-8</sup> bond strength between biological receptors/ligands,<sup>9</sup> and, more recently, strength of a single covalent bond.<sup>10</sup> Nevertheless, due to its intrinsic prin-

ciple relying on the use of a soft cantilever acting as a spring, one cannot control the distance between the end-to-end terminations of the probed species. This major drawback leads to a convolution effect in the force/distance curves measured and explains the undesirable instability (arrows in Fig. 1) taking place when the gradient of attractive forces exceeds the spring constant of the cantilever. As a result, when measuring bond strength, a very informative part of the force profile remains obscured. If one wants to go a step further in the understanding of the mechanism involved when doing force spectroscopy measurements, one must move toward a new force sensor radically different in its principle to measure forces. Hence, to inspect more closely this unexplored region, we used a recently developed instrument named the magnetic levitation force microscope (MLFM). This original force balance was previously illustrated by its remarkable and powerful ability to depict the entire range of a force profile, even in the presence of attractive forces.<sup>11</sup> Its principle relies on precisely controlling and imposing the tip/sample distance, and therefore the end-to-end distance of the species probed. This can be realized by compensating for all

<sup>a)</sup>Authors to whom correspondence should be addressed.

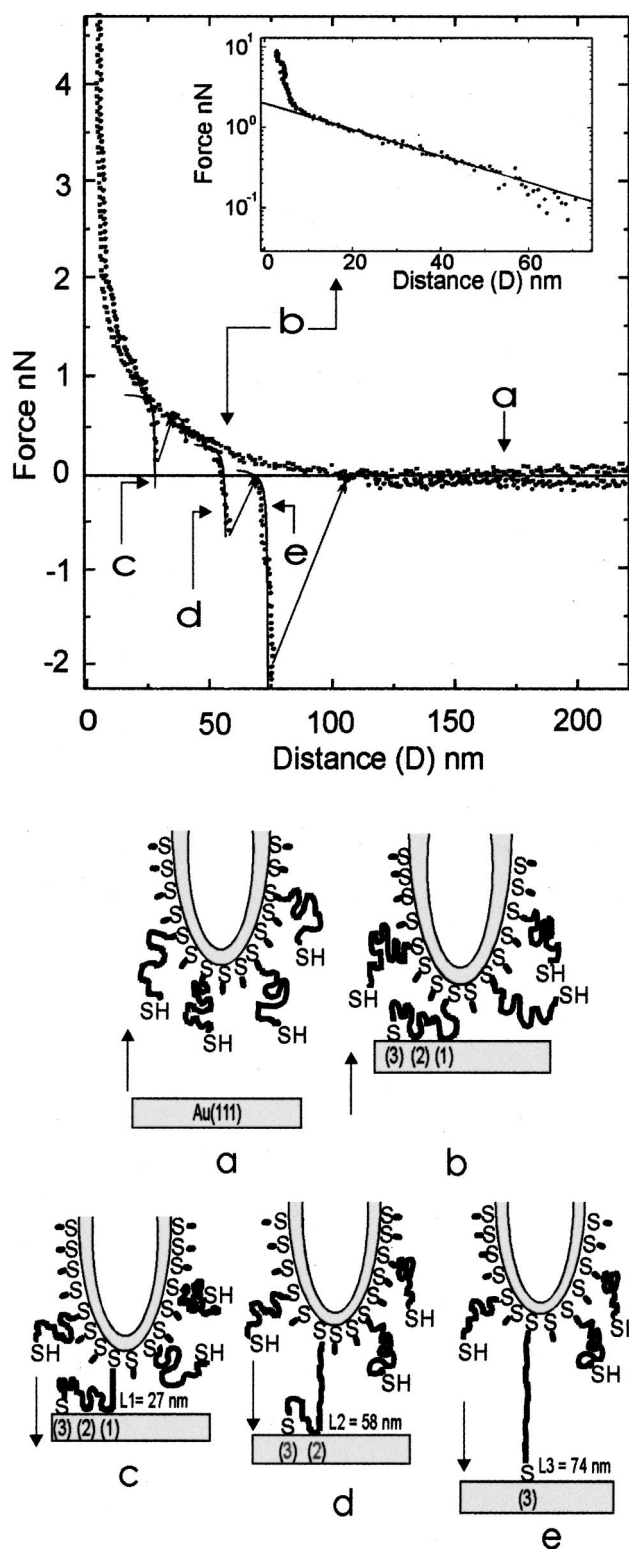


FIG. 1. Force/distance curve obtained when using a conventional AFM. The squares represent the approach of the modified tip to the surface. (a) The tip is far away from the surface: no interaction is observed. (b) Compression of the coils plotted on log scale in the inset (Refs. 20, 21). After a certain repulsive force threshold, the movement of the surface is reversed (dots). (c) and (d) Stretching of sections of single polymer chain, which is tethered to the surface via physical adsorption of its segments (the trains).  $L_1 = 27$  nm and  $L_2 = 58$  nm are the lengths associated with the parts of the polymer chains being stretched. (e) Full elongation of the chain ( $L_3 = 74$  nm) stretched through its extremities, which are tethered to the surface and the tip by covalent bonds (Au-S).

forces acting on the tip by means of an electromagnetic system and a built-in servo loop.<sup>12,13</sup> The measured distance corresponds now to the true distance separating the tip and the surface, and forces are equilibrated at any moment. The only noticeable drawback of this apparatus is its lower force resolution ( $\approx 500$  pN) compared to the usual AFM.

## II. EXPERIMENT

### A. Polymer synthesis

PMAA, substituted at both ends with thiol groups (HS-PMAA-SH), was synthesized via living free-radical polymerization according to the procedure described by Otsu *et al.*<sup>14</sup> To obtain HS-PMAA-SH, *p*-xylylene-bis(*N,N*-diethyldithiocarbamate) (XDC) was used as a bi-functional initiator; the thiocarbamate-functional PMAA was subsequently hydrolyzed with KOH, converting it to HS-PMAA-SH.

### B. Tip preparation

Coadsorption of HS-PMAA-SH and 12-mercapto-1-dodecanol onto a gold-coated tip provides a spontaneously formed mixed monolayer in which the polymer is randomly distributed.<sup>15</sup> By changing the relative concentration of species, the grafting density of polymer chains onto the gold surface can be easily adjusted. Furthermore, the use of 12-mercapto-1-dodecanol limits the formation of loops that occurs when only HS-PMAA-SH is used.<sup>16</sup> Hence only one thiol group at one end of the polymer chain is covalently bonded (Au-S) onto the tip, the other thiol being free to spontaneously form an Au-S bond when a bare gold surface is approaching. HS-PMAA-SH chains in the presence of pure water swell and expose their reactive sites (thiol groups) to the surrounding medium.

### C. Conventional AFM

In the conventional AFM, the vertical displacement of the cantilever is measured by means of the laser beam deflection technique and, via its spring constant, is correlated with the forces exerted between the modified tip (integrated on the cantilever) and the bare gold surface. The force/distance curves presented here have been deconvoluted<sup>1</sup> to obtain the true force profile, since the distance recorded by AFM corresponds to the displacement of the piezo and does not take into account the displacement of the tip, which also moves during measurements due to the finite stiffness of the cantilever.

### D. Magnetic levitation force microscopy

The principle of the MLFM is based on exerting a vertical magnetic force, by circulating an electric current through a coil, on a small samarium cobalt magnet. This magnetic force balances continuously the sum of all forces exerted on the magnet via the integrated tip. The design of the magnetic field ensures the radial stability of the equilibrium. In the vertical direction a feedback loop [proportional integral differential (PID)], associated with an optical position sensor, drives the current through the coil and ensures

stability better than 0.05 nm.<sup>12</sup> Thus, the magnet is placed in levitation without contact with the surrounding medium. The measurement of the current circulating through the coil gives direct information on the forces exerted between the modified tip and a surface displaced from below by using a piezoelectric device (0.0866 nm between two steps, i.e., two points on the curve presented). The magnet can be placed in air or liquid. A computer drives the displacement of the surface and records simultaneously and in real time (DSP acquisition card) the value of the current, which is directly translated into force.

### III. RESULTS AND DISCUSSION

#### A. Results obtained with conventional AFM

Figure 1 represents a typical force/distance curve, obtained with the conventional AFM, using a PMAA having an average degree of polymerization  $\bar{N}_n = 275$  and an estimated grafting density  $\sigma = 1500 \mu\text{m}^{-2}$ . During the approach, one can only see the gradual increase of the loading force due to the compression of the polymer chains, which can be modeled using the formula<sup>17,18</sup>

$$F(d) \approx \frac{100RL_0k_bT}{s^3} \exp(-2\pi d/L_0), \quad (1)$$

where  $R$  is the radius of curvature of the gold-coated tip (125 nm),  $L_0$  the size of the polymer layer,  $s$  the mean distance between the grafting points of the chains (i.e.,  $s = \sigma^{-0.5}$ ),  $k_b$  the Boltzmann constant ( $1.381 \times 10^{-23} \text{JK}^{-1}$ ) and  $T$  the temperature (298 K). The fitting of the curve<sup>19–21</sup> for  $0.2 < d/(2L_0) < 0.9$  (see inset in Fig. 1) allows the determination of  $L_0 \approx 150$  and  $s \approx 16$  nm, values which are consistent with those obtained using AFM images,<sup>15,22</sup> even if they are somewhat larger than the expected ones as noticed by others.<sup>18</sup> It nevertheless confirms that a self-assembling monolayer is formed with a grafting density allowing the observation of single-molecule force events.

On the receding force/distance curve, we observe several occurrences of attractive interactions, not present during the approach. These events signal the bridging interaction of the polymer onto the bare gold surface. When trying to separate the two surfaces, the trapped polymer chain exerts a restoring force on the cantilever through the tip via its anchoring points on both surfaces. This force is mainly governed by the entropic response of the polymer chain and the resulting events can be fitted using entropic elasticity models, such as the freely jointed chain (FJC) model,<sup>23</sup>

$$F(d) = \frac{k_bT}{l_k} \mathcal{L}^* \left( \frac{d}{L_i} \right), \quad (2)$$

where  $\mathcal{L}^*$  is the inverse Langevin function,  $L_i$  the contour length of the part of the chain being stretched, and  $l_k$  the Kuhn length, which is twice the length of one monomer unit for PMAA. Thus, replacing the parameters by their theoretical values, and merely by adjusting the value of  $L_i$  for each event [ $L_1$ ,  $L_2$ ,  $L_3$  in Figs. 1(c)–1(e)], one can easily fit all these events (solid lines in Fig. 1), and confirm their entropic nature. Ultimately, when the force exerted on the cantilever

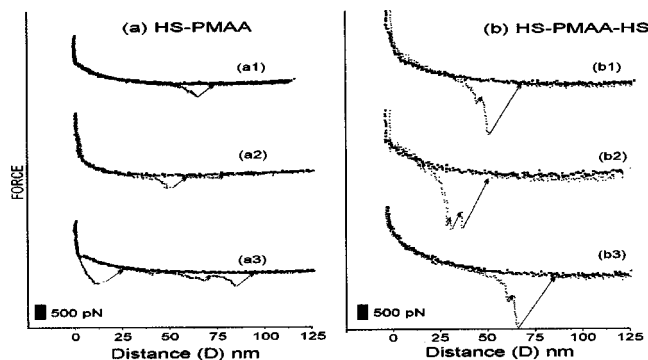


FIG. 2. Difference in force/distance curves between polymers tethered from one or two thiol groups. Arrows correspond to the instabilities of the cantilever, the squares correspond to the approach, the dots to the receding movement. Figures (a1), (a2), and (a3) represent the force-distance curves obtained with PMAA bearing only one thiol group: only the adsorption effect (a few 100 nN) can be observed. Figures (b1), (b2), and (b3), show the force profiles observed when using PMAA bearing two thiols groups. The terminal force value of 2.2 nN is associated with the rupture of a single covalent bond in the system.

exceeds the bridging force anchoring the polymer onto the surface, detachment of the polymeric chain occurs, leading to the cantilever instability described before.

One may notice that the interactions fall within two distinct force-ranges during these force spectroscopic measurements, strongly suggesting two types of polymer/surface interactions involved in the bridging process. The first kind (i.e., events associated with  $L_1$  and  $L_2$ ) lies within a force range of 200 to 600 pN. The magnitude of these forces typically corresponds to a physisorption process of polymer segments with random length (trains) onto the bare gold surface. The random number of these events depends on the number of adsorbed sites within the polymer coil, a loop being formed between two adsorbed sites.<sup>1</sup> The other kind of force has a well-defined amplitude of about 2.2 nN, as observed on many force/distance curve profiles [Fig. 2(b)]. This type of interaction always appears as the last event in the receding part of the force profile ( $L_3$ ). If one considers that the polymer chain we used has the ability to make a covalent bond with the bare gold surface via its free thiol end group ( $-\text{SH}$ ), the nature of these terminal events can easily be explained: all the adsorbed sites being removed, one has actually stretched the chain via its two covalently bonded extremities. This time, the force has to overcome an important maximum value, to liberate the two surfaces: a covalent bond must break at some point. Therefore, the terminal rupture value of 2.2 nN can be directly associated with the cleavage of a single covalent bond occurring at a fraction of full chain extension  $d/L_i = 0.998$ . In a very small number of cases it appears that one has stretched several polymer chains via their extremities during one experiment, as illustrated in Fig. 2(b2). As a result of the high polydispersity of the polymer used, drastically limiting the possibility of stretching two chains of the same contour length at the same moment, each event appears well separated from the others, allowing its individual recognition, and revealing the reproducibility of the force-value involved during the rupture of a single covalent bond. To confirm the covalent nature of these events, we

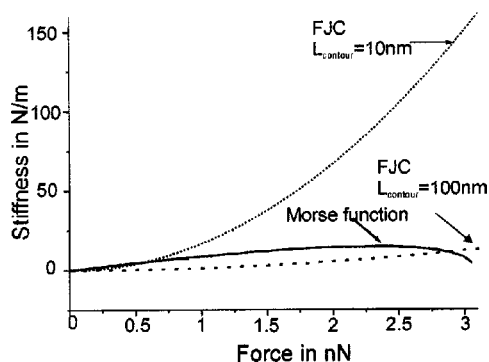


FIG. 3. Comparison of the stiffness of the covalent bond and entropic elasticity as a function of applied force. The stiffness of the Morse function was plotted only for distance  $(\delta x) > (\delta x_{\max} = \text{elongation corresponding to } F_{\text{maximum}})$ , which corresponds to the region where instabilities can occur. The parameters used are:  $\beta = 0.96 \times 10^{10} \text{ m}^{-1}$ ,  $D_e = 0.641 \text{ aJ}$ . Two contour lengths were used for the FJC function (10 and 100 nm).

performed blank experiments with polymer chains bearing only one thiol group [Fig. 2(a)]. In this case, free thiol groups are no longer available for covalent bonding with the bare gold surface. The measured force profiles exhibit only the adsorption effect described previously. This supports the previous assumption that the polymer chains can be stretched via their covalently bonded extremities, and that the measured value of 2.2 nN is indeed directly correlated with the rupture of a covalent bond.

## B. Results obtained with the MLFM

In order to further investigate this bond rupture process we used the MLFM as a molecular tensile tester. But, if one wants to map out the entire force profile associated with the rupture of a single bond, one must take care of the polymer length used when performing such experiments. In fact, as shown previously, another effect is operative during the cleavage of the bond: the entropic elasticity of the polymer chains, acting as a nonlinear spring. Hence, despite the stability of the system used to measure forces, instability can occur due to this uncontrollable external elasticity: the polymer will jump out of contact if its entropic elasticity is lower than the stiffness involved during the rupture of the covalent bond. Measurements using the usual AFM allowed us to precisely determine all the parameters playing a role in the entropic elasticity. For a proper evaluation of this effect, one must compare the function that describes the stiffness of the covalent bond (Morse function) to the one describing the entropic elasticity of the polymer chain (FJC function), which strongly varies with contour length and chain extension. In order to allow this comparison and to get rid of the distance dependencies, one can plot the stiffness of these two models as a function of the applied force as shown in Fig. 3. One can easily deduce from this figure that long polymer chains ( $\approx 100 \text{ nm}$ ) cause instabilities occurring around the maximum force-value needed to cleave a covalent bond. If one chooses a smaller polymer length ( $\approx 10 \text{ nm}$ ), the force profile associated with the cleavage of the bond can be recorded when using a force sensor stable in position such as the MLFM. To fulfill this condition, we synthesized a shorter

polymer ( $\bar{N}_n = 55$ ). To limit the amount of polymer tethered, we also decreased the grafting density ( $\sigma = 400 \mu\text{m}^{-2}$ ), the radius of the electrochemically etched tip being larger ( $\approx 300 \text{ nm}$ ) than the one used with the standard AFM. Figure 4 represents an example of the interaction observed with MLFM according to the above experimental conditions. The approach [Fig. 4(a)] does not reveal any particular behavior except the contact point between the two surfaces. One notices that due to the use of a low grafting density and short polymer chains, the exponential increase corresponding to the compression of the chains cannot be distinguished from the noise. During the receding movement [Fig. 4(b)], a relatively long-range interaction ( $\approx 6 \text{ nm}$ ) takes place at short separation distance. This interaction can be fitted with a  $-1/d^2$  law and can be associated with the van der Waals (vdW) force between the tip and the surface<sup>24</sup> ( $F_{\text{v.d.w.}} = -AR/6d^2$ ,  $A = \text{Hamaker constant} = 1.8 \times 10^{-19} \text{ J}$  for the fit). As previously observed with standard AFM [Fig. 2(a3)], this interaction does not appear during the approach. This can be explained by assuming that the polymer chains screen this interaction during the compression part, or that they are displaced laterally,<sup>25</sup> leaving a gap for the two gold surfaces to interact with each other when retracting. Beyond this van der Waals interaction, the force remains zero for a few nm and one may notice that the adsorption effect described before (few 100 pN) cannot be distinguished from the noise. We then see four sharp events, randomly distributed, indicating that the polymer chain is linked to both surfaces and exerts a restoring force on the tip. Considering the noise level of the MLFM (0.5 nN), the magnitude of the force associated with these events (2.6 nN) is comparable to the results obtained with the conventional AFM when rupturing a single covalent bond. It is therefore more than likely that all these events have the same origin as those previously observed: the breakage of four covalent bonds from four distinct tethered polymer chains. Due to the high polydispersity in the length of the polymer chains and the short-range interaction of these events ( $\approx 0.6 \text{ nm}$ ), each appears well-separated from the others, allowing individual peak analysis.

To confirm the covalent nature of these events, we fitted several attractive peaks with a Morse force function, which describes a covalent bond, as shown by the dashed lines in Figs. 4(b) and 4(c). The general equation for this function is

$$F_{\text{Morse}} = -\frac{\partial}{\partial d} V_{\text{Morse}} = 2\beta D_e [\exp(-2\beta \delta x) - \exp(-\beta \delta x)], \quad (3)$$

where  $D_e$  is the dissociation energy,  $\beta$  is called the Morse  $\beta$  parameter, and  $\delta x$  is the deviation from the equilibrium distance of the bond. We found  $D_e = 0.641 \text{ aJ}$  and  $\beta = 0.96 \times 10^{10} \text{ m}^{-1}$ . The value of  $D_e$  is typically in the range of the dissociation energy for covalent bonds. The value of  $\beta$  can be related to the stiffness  $k_s$  of the bond at its equilibrium position ( $\delta x = 0$ ) as  $\beta = (k_s/2D_e)^{0.5}$ . We obtain experimentally a value for  $k_s = 118 \text{ N/m}$ , which lies on the low side of the stiffness range for a typical covalent bond ( $\approx 250\text{--}500 \text{ N/m}$ ).

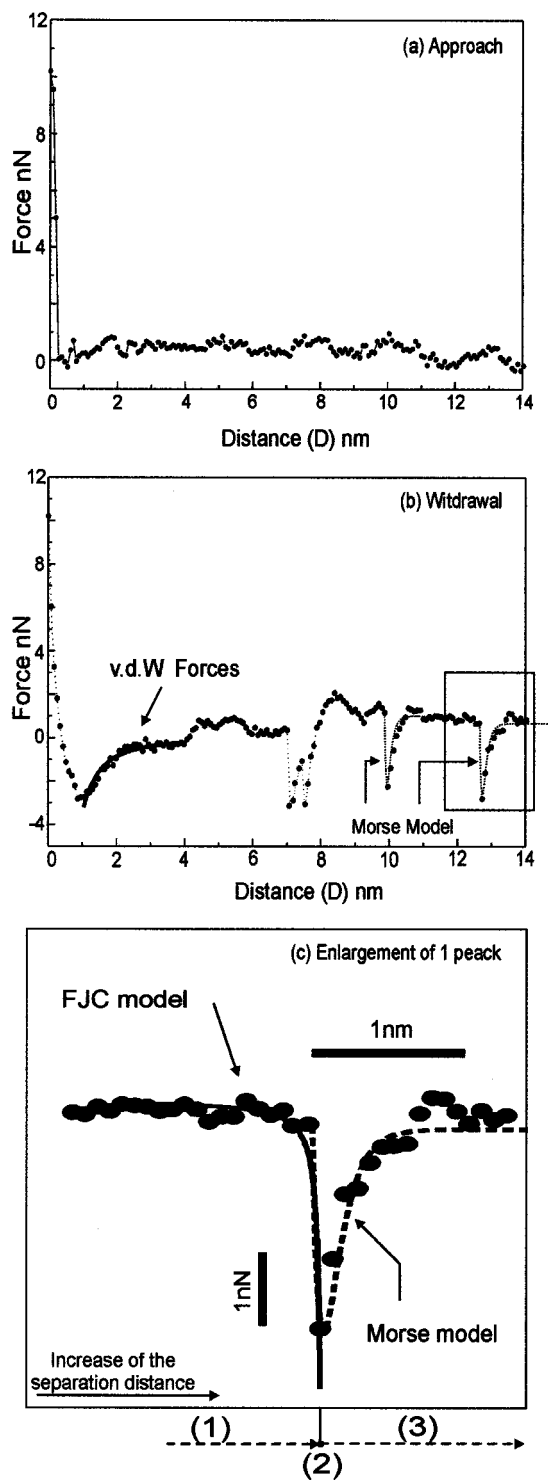


FIG. 4. Force/distance curve obtained with MLFM, showing the force profile associated with the cleavage of a covalent bond. (a) Approach of the two surfaces. (b) Withdrawal of the surfaces. The black line corresponds to the fit using a van der Waals function (Hamaker constant found =  $1.8 \times 10^{-19}$  J), the dotted lines represent the Morse function ( $\beta = 0.96 \times 10^{10} \text{ m}^{-1}$ ;  $D_e = 0.641 \text{ eV}$ ). (c) Enlargement of one peak: (1) at low force value, entropic stiffness ( $L_{\text{contour}} = 12.5 \text{ nm}$ ) rules the force profile; when the force drastically increases, the measured profile is a combination of the entropic effect and the bond rupture process; (2) the force reaches a maximum ( $F_{\text{maximum}}$ ), the stiffness of the bond drops to zero; (3) in this region where the stiffness of the bond is inferior to the entropic one (see Fig. 3), the force profile mainly reflects the bond rupture process.

The enlargement of one peak, represented in Fig. 4(c), reveals the force profile measured during this cleavage process. This profile is in fact dominated by a combination of two events taking place simultaneously: the entropic elasticity, and the force associated with the rupture of a single bond, acting in series. For a comparison of the effects, the two models associated with these events are superimposed on the data points. On the left part of the curve (1), the force profile is mainly dominated at low forces by the low stiffness of the entropic elasticity. When the polymer chain reaches its contour length (12.5 nm) close to point (2), the sudden increase of the nonlinear entropic elasticity stiffness, together with the comparable high stiffness of the bond involved in the rupture process ( $> \text{few } 100 \text{ nN/nm}$  for forces  $< F_{\text{maximum}}$  to cleave the bond), causes an abrupt change in the force profile (from 0 to 2.9 nN in less than 0.16 nm). At point (2), when the force has reached this maximum value, the stiffness of the bond being cleaved drops suddenly down to zero and then remains lower than the stiffness of the entropic elasticity in the rest of the force profile (see Fig. 3). This explains that the bond rupture process mainly dominates this region (3) of smooth force decrease, the entropic elasticity giving only a slight convolution effect over the total distance measured by the MLFM. One can easily calculate the total retraction length of the polymer chain (0.07 nm) in this region, which extends over about 0.6 nm. The noise level of the MLFM limiting mainly the precision of the fit, this minor retraction effect was neglected during the fit and the curves presented were not deconvoluted.

### C. Density functional quantum calculations

In order to gain some insight into which bond actually breaks first in these experiments, we have performed a series of density functional electronic structure calculations with the ADF program package<sup>26,27</sup> using the BLYP density functional. To get a representative value for the rupture force of each of the bonds present in the oligomers studied, we analyzed the rupture of the weakest bond in the suite of molecules  $\text{Au-S(CH}_2)_2\text{-H}$ ,  $\text{H-S(CH}_2)_2\text{-H}$ ,  $\text{H-(CH}_2)_3\text{-H}$  and  $\text{Au}_2$  in which, respectively, the Au-S, S-C, C-C and Au-Au bond breaks first. The rupture force was determined by first optimizing the equilibrium geometry and then performing a series of calculations where the end atoms were fixed at increasingly larger distances (in steps of 0.1 Å out to a stretch of 4 Å) while all other atoms relaxed to their (strained) equilibrium positions. The force on the end atoms was then calculated (using the analytical gradients determined by ADF) and plotted as a function of elongation after which the maximum force, i.e., the rupture force could easily be determined. The results are given in Table I. In all cases the main backbone was constrained to be flat. We also repeated the calculations with longer oligomers  $\text{Au-S(CH}_2)_4\text{S-Au}$ , which led to identical rupture forces for the Au-S bond, thus verifying that oligomer length is not important for this property.

In the case of the Au-containing compound it is essential to include the effects of the theory of relativity into the calculation as has been well known for quite some time<sup>28</sup> and is also evident from the large relativistic corrections in Table I.

TABLE I. Comparison of the maximum force value to rupture of various single covalent bonds, determined by density functional quantum calculations.

Bond	Relativistic	Nonrelativistic
Au-S	2.7 nN	2 nN
Au-Au	2.5 nN	1.5 nN
S-C	3.7 nN	3.7 nN
C-C	6.0 nN	6.0 nN

The method used was the scalar ZORA method described before.<sup>29</sup> Relativity usually leads to a bond shortening as well as a stabilization in these cases,<sup>28</sup> both leading to an increase of the maximum force in the Au-containing bond. These effects are understood<sup>28</sup> to be a consequence of the relativistic increase in mass of the valence electron with velocity, which can be substantial for the 6*s* valence electron of Au when it is close to the highly charged Au nucleus.

As a result of these calculations (see Table I), C-C and S-C bonds can definitively be ruled out, the maximum force needed to break these bonds being, respectively, 6.0 and 3.7 nN, far above the experimental values. The only two remaining bonds are the Au-Au (removing one gold atom from the surface) or Au-S bonds, both residing at the extremities of the polymer chain. Calculations can easily determine the Au-S bond force maximum value. The value of 2.7 nN found is consistent with the experimental value observed. Concerning the gold-gold bond, it is difficult to model the entire gold surface to determine the rupture force involved when one gold atom is removed away from it. To simplify the calculations for this bond, we have then chosen the simplest possible representation, namely a dimer. A value of 2.5 nN was found for this bond, which is also in the range of the measured values. However, it is entirely possible that this calculated value is underestimated since all the interactions from other gold atoms in/on the surface are not taken into account. One cannot therefore completely determine at this stage of knowledge, which bond of these two is the more likely to break, but one can definitely affirm that the rupture takes place in close proximity to the gold surface. This implies that the one atom staying on the polymer chain during this separation process will feel the van der Waals interaction of the nearby gold surface. This could explain and support that the measured profile obtained with MLFM extends over a slightly longer range ( $\approx 0.6$  nm) than expected ( $\approx 0.4$  nm), resulting in an underestimation of the  $k_s$  value when fitting the curve with a simple Morse model.

#### IV. CONCLUSIONS

We demonstrated that conventional AFM has the ability to determine the rupture force of a covalent bond. Using its high force sensitivity, we determined various relevant parameters from entropic elasticity force measurements on tethered PMAA. From these constants, we were able to predict a suitable polymer length required to take full advantage of the stability of a new force sensor named MLFM. This apparatus, used as a microscopic molecular tensile tester, confirmed the value previously obtained with the conven-

tional AFM, and allowed us to map out, in a direct way, the entire force profile associated with the cleavage of a single covalent bond. By fitting this profile, we obtained fundamental spectroscopic constants, which are currently only accessible through vibrational spectroscopy experiments. These experimentally determined constants lie within the range of those already known for covalent bonds. Calculations reveal that the atoms involved in the rupture process obviously belong to the extremities of the tethered polymer chain, even if one cannot definitely settle which of the Au-Au or Au-S bonds is breaking. If MLFM can be made to have the sensitivity of the classical AFM, its ability to map out the entire force profile associated with the cleavage of a single bond will give us a great opportunity in the development of our theoretical understanding of one of the most important elementary interactions present everywhere in nature: the covalent bond.

#### ACKNOWLEDGMENTS

This work was supported by ULTIMATECH (CNRS), the Netherlands Foundation for Fundamental Research on Matter (FOM), the Netherlands Foundation for Chemical Research (NWO-CW) and the Netherlands Organization for Scientific Research (NWO). The TMR EU individual's fellowship for Lionel Garnier is gratefully acknowledged. One of us, L.G., thanks the "Rotary club de Besançon" for its financial support. We finally thank Dr. V. Koutsos for his early experimental involvement, M. Doreau for his active participation in the realization of the MLFM and P. F. van Hutten for his careful reading of the manuscript.

- <sup>1</sup>C. Ortiz and G. Hadziioannou, *Macromolecules* **32**, 780 (1999).
- <sup>2</sup>M. Rief, J. Pascual, M. Saraste, and H. E. Gaub, *J. Mol. Biol.* **286**, 553 (1999).
- <sup>3</sup>J. E. Bemis, B. B. Akhremitchev, and G. C. Walker, *Langmuir* **15**, 2799 (1999).
- <sup>4</sup>H. Li, B. Liu, X. Zhang, C. Gao, J. Shen, and G. Zou, *Langmuir* **15**, 2120 (1999).
- <sup>5</sup>M. Maaloum and A. Courvoisier, *Macromolecules* **32**, 4989 (1999).
- <sup>6</sup>M. Rief, M. Gautel, A. Schemmel, and H. E. Gaub, *Biophys. J.* **75**, 3008 (1998).
- <sup>7</sup>M. Rief, P. Schulz-Vanheyden, and H. E. Gaub, *NATO Adv. Study Inst. Ser., Ser. E* **348**, 41 (1998).
- <sup>8</sup>M. Rief, F. Oesterhelt, B. Heymann, and H. E. Gaub, *Science* **275**, 1295 (1997).
- <sup>9</sup>E.-L. Florin, V. T. Moy, and H. E. Gaub, *Science* **264**, 415 (1994).
- <sup>10</sup>M. Grandbois, M. Beyer, M. Rief, H. Clausen-Schaumann, and H. E. Gaub, *Science* **283**, 1727 (1999).
- <sup>11</sup>B. Gauthier-Manuel, *Europhys. Lett.* **17**, 195 (1992).
- <sup>12</sup>B. Gauthier-Manuel and L. Garnier, *Rev. Sci. Instrum.* **68**, 2486 (1997).
- <sup>13</sup>B. Gauthier-Manuel and L. Garnier, *Surf. Interface Anal.* **27**, 287 (1999).
- <sup>14</sup>T. Otsu, T. Matsunaga, A. Kuriyama, and N. Oshioaka, *Eur. Polym. J.* **25**, 643 (1989).
- <sup>15</sup>V. Koutsos, E. W. van der Vegte, E. Pelletier, A. Stamouli, and G. Hadziioannou, *Macromolecules* **30**, 4719 (1997).
- <sup>16</sup>M. Niwa, M. Shimoguchi, and N. Higashi, *J. Colloid Interface Sci.* **148**, 592 (1992).
- <sup>17</sup>J. N. Israelachvili, *Intermolecular and Surface Forces* (Academic, London, 1992).
- <sup>18</sup>S. J. O'Shea, M. E. Welland, and T. Rayment, *Langmuir* **9**, 1826 (1993).
- <sup>19</sup>S. Alexander, *J. Phys. (France)* **38**, 977 (1977).
- <sup>20</sup>P. G. de Gennes, *C. R. Acad. Sci., Ser. II: Mec., Phys., Chim., Sci. Terre Univers.* **300**, 839 (1985).
- <sup>21</sup>P. G. de Gennes, *Adv. Colloid Interface Sci.* **27**, 189 (1987).
- <sup>22</sup>V. Koutsos, E. W. van der Vegte, P. C. Grim, and G. Hadziioannou, *Macromolecules* **31**, 116 (1998).



- <sup>23</sup>A. Grosberg and A. R. Khokhlov, *Statistical Physics of Macromolecules* (AIP, Woodbury, NY, 1994).
- <sup>24</sup>The Hamaker constant found ( $1.8 \times 10^{-19}$  J), is a reasonable value, but difficult to compare to a theoretical one since the system used is complex (polymer+water+12-mercapto-1-dodecanol+gold).
- <sup>25</sup>G. Subramanian, D. R. M. Williams, and P. A. Pincus, *Europhys. Lett.* **29**, 285 (1995).
- <sup>26</sup>C. Fonseca Guerra, O. Visser, J. G. Snijders, G. te Velde, and E. J. Baerends, *Methods and Techniques in Computational Chemistry*, edited by E. Clementi and G. Corongiu (STEF, Caligari, Strasbourg, 1995), p. 305.
- <sup>27</sup>C. Fonseca Guerra, J. G. Snijders, G. te Velde, and E. J. Baerends, *Theor. Chem. Acc.* **99**, 391 (1998).
- <sup>28</sup>T. Ziegler, J. G. Snijders, and E. J. Baerends, *J. Chem. Phys.* **74**, 1271 (1981).
- <sup>29</sup>E. van Lenthe, R. van Leeuwen, E. J. Baerends, and J. G. Snijders, *Int. J. Quantum Chem.* **57**, 281 (1996).